Resonance Effect for Neural Spike Time Reliability

JOHN D. HUNTER,[1] JOHN G. MILTON,[1,3] PETER J. THOMAS,[2] AND JACK D. COWAN[2,3]
[1]*Committee on Neurobiology,* [2]*Department of Mathematics, and* [3]*Department of Neurology, The University of Chicago, Chicago, Illinois 60637*

Hunter, John D., John G. Milton, Peter J. Thomas, and Jack D. Cowan. Resonance effect for neural spike time reliability. *J. Neurophysiol.* 80: 1427–1438, 1998. The spike timing reliability of *Aplysia* motoneurons stimulated by repeated presentation of periodic or aperiodic input currents is investigated. Two properties of the input are varied, the frequency content and the relative amplitude of the fluctuations to the mean (expressed as the coefficient of variation; CV). It is shown that, for small relative amplitude fluctuations (CV $\approx$ 0.05–0.15), the reliability of spike timing is enhanced if the input contains a resonant frequency equal to the firing rate of the neuron in response to the DC component of the input. This resonance-related enhancement in reliability decreases as the relative amplitude of the fluctuations increases (CV $\rightarrow$ 1). Similar results were obtained for a leaky integrate-and-fire neuronal model, suggesting that these effects are a general property of encoders that combine a threshold with a leaky integrator. These observations suggest that, when the magnitude of input fluctuations is small, changes in the power spectrum of the current fluctuations or in the spike discharge rate can have a pronounced effect on the ability of the neuron to encode a time-varying input with reliably timed spikes.

INTRODUCTION

Considerable effort was devoted to measuring and modeling the statistical properties of spike trains generated by neurons in response to known stimuli (Otmakhov et al. 1993; Perkel and Bullock 1968). An unsettled question is which properties of the output neural spike train encode the information concerning the neuron's input (Geisler et al. 1991; Softky 1995). Candidate neural codes include the mean rate of firing (Redman et al. 1968), the distribution of interspike firing times (Sanderson et al. 1973; Werner and Mountcastle 1963), pattern of spikes (Middlebrooks et al. 1994; Optican and Richmond 1987; Segundo et al. 1966;), and the precise times that the neuron fires (Hopfield 1995; Mainen and Sejnowski 1995). A precondition of a spike time code is that the times of response to an input signal be reliable in the presence of noise (Calvin and Stevens 1968; Fatt and Katz 1950). However, neuronal responses are notoriously variable, and this variability was the source of long-standing interest (Croner et al. 1993; Geisler and Goldberg 1966; Holt et al. 1996; Softky and Koch 1993; Stein 1965; Wilbur and Rinzel 1983; Wu et al. 1994). In the visual cortex, this variability reflects ongoing cortical activity (Arieli et al. 1996) and the influence of eye movements (Gur et al. 1997).

A recently emphasized experimental paradigm concerns the measurement of the reliability of spike timing when a neuron is repeatedly given the same time-varying input. Precisely timed spike trains are produced by neurons in response to aperiodic input signals in which current fluctuations resemble synaptic activity (Mainen and Sejnowski 1995; Nowak et al. 1997; Tang et al. 1997), in contrast to those produced by a constant current stimulus. Precise spike time responses are also observed in motion-sensitive neurons in response to time-varying visual stimuli in the fly (de Ruyter van Steveninck et al. 1997). These results suggest that the intrinsic noise in the spike-generating mechanism is low relative to the intensity of the fluctuating input currents.

In interpreting these results, an important consideration is the magnitude of the fluctuations in the input relative to the current necessary to cause neuronal spiking. It is not difficult to appreciate that spike timing will be reliable when the relative magnitude of the input fluctuations is high. In the presence of noise, the width of interspike interval (ISI) distribution is inversely proportional to the slope of the membrane potential (dV/dt) at threshold (Goldberg et al. 1984; Stein 1967b). A current with a large amplitude fluctuating component will cause threshold crossings with a steeper slope than will a constant current and thus generate more reliably timed spikes in the presence of noise. An analogous slope condition exists for the synchronization of a network of neurons to a coherent input (Gerstner et al. 1996).

However, in many situations, the fluctuating component of the input is relatively small (Calvin and Stevens 1968; Church and Lloyd 1994; Steriade 1997; Steriade et al. 1993; Wilson and Kawaguchi 1996). Here we show that even under these conditions it is possible for the spike timing to be reliable through a resonance phenomenon (Fig. 1). An input signal may be divided into two components, a DC component and a time-varying component. The neuron's firing rate (f_{DC}) in response to the DC component places constraints on the types of signals that may be encoded with reliably timed spikes in the presence of noise. Suppose at *time 0* a spike occurs on the rising phase of an input signal and the membrane potential is reset to rest. If the time-varying component of the input is small compared with the DC component, then the next spike will not occur until some time approximately equal to T_{DC}, the inverse of the f_{DC}. If the time-varying component of the input signal is increasing around time T_{DC}, the spike time distribution will be narrower than if the time-varying component is decreasing at this time because of slope considerations. Thus we expect small-amplitude periodic signals that are modulated at a frequency f_{DC} or its harmonics to generate more reliably timed spike trains than other frequencies. A number of theoretical investigations and experimental observations of neurons and neural models with periodic inputs noted the importance of f_{DC} in generating phase-locked firing patterns (Keener et al. 1981; Knight 1972a,b; Rescigno et al. 1970; Scharstein

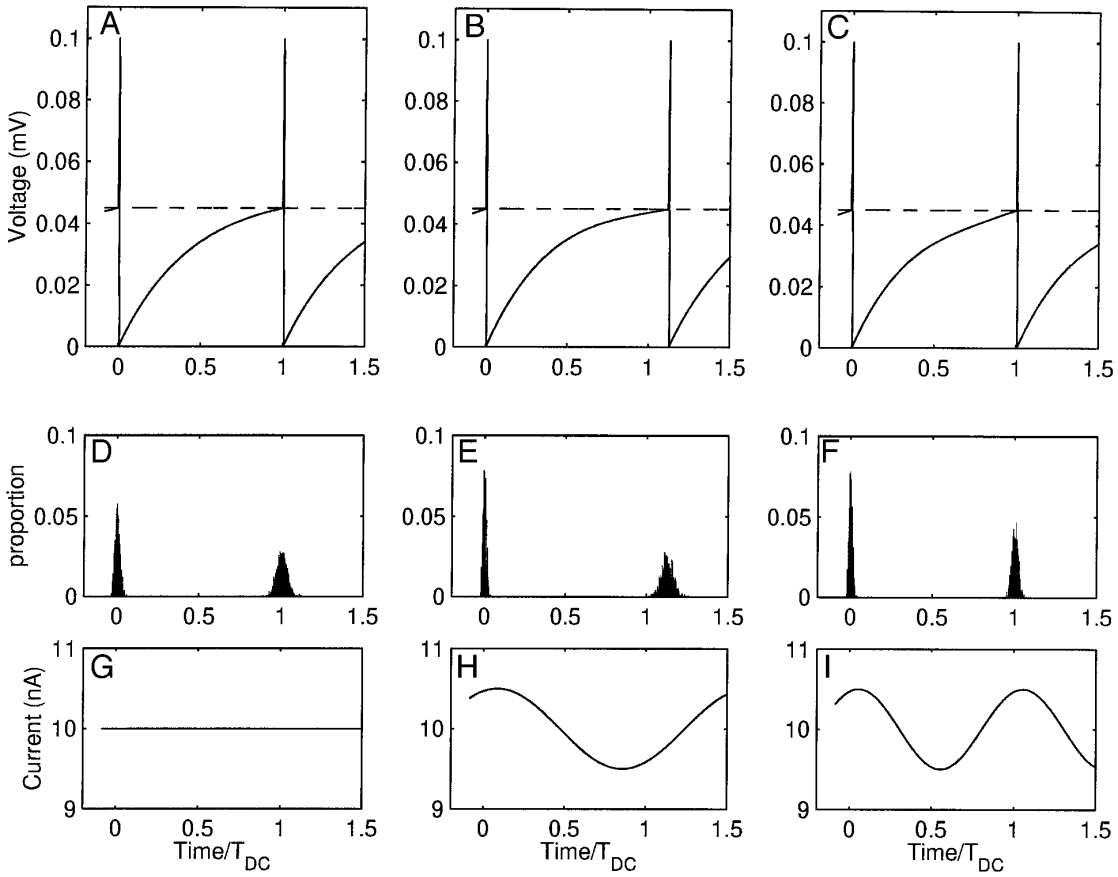

FIG. 1. Leaky integrate and fire model with constant and periodic inputs. *A*: membrane potential in response to a DC input current. *B*: membrane potential trajectory with input current modulated at $f/f_{DC} = 0.65$. *C*: trajectory when $f/f_{DC} = 1.0$. Dashed lines in *A–C* indicate the threshold for spiking. *D–F*: distribution of spike times for 1,000 presentations of the currents shown in *G–I* in the presence of noise. For each of the 3 inputs, initial conditions were chosen to trigger a spike at *time 0* in the absence of noise, resulting in a peaked spike time distribution around 0 when noise is added. Note that the 1st peak in the spike distribution is sharper in response to the sinusoidal currents (*E* and *F*) than in response to a DC input (*D*) because the slope of the membrane potential at threshold crossing is steeper; the initial conditions were chosen so that the 1st spike in the deterministic case would occur at the same phase of the sinusoids. At the 2nd threshold crossing, the slope of the membrane potential trajectory in *C* is steeper than in *A* or *B*, which causes a narrower spike time distribution in the presence of noise (*D–F*). The input currents are shown in *G–I*. See text for discussion. $\mu = 10$ nA, $m = 0.05$, $f_{DC} = 8.7$ Hz, $\phi = 1.22$, $R = 5$ MΩ, $C = 10$ nF, $\theta = 45$ mV, and $\sigma_n = 40$ nA; for *A*, *D*, and *G*, $m = 0$.

1979). However, the possibility that f_{DC} plays a fundamental role in shaping the response of neurons to aperiodic inputs was not investigated.

Here we demonstrate that spike time reliability in response to aperiodic signals depends on the frequency content and modulation amplitude of the input and the f_{DC} of the neuron. The results are presented in three sections. The first section describes spike timing reliability when sinusoidal inputs are repeatedly presented to a slowly adapting *Aplysia* buccal motoneuron. This section shows the dependence of spike timing reliability on the frequency content of the input signal and f_{DC} for periodic inputs. The second section examines spike timing reliability when the neuron repeatedly receives a set of aperiodic signals. This section demonstrates that spike timing reliability is lowest when the aperiodic signal does not contain frequencies around and including f_{DC} and highest when it does. Finally, the third section demonstrates that all of these experimental observations can be readily accounted for by a leaky integrate and fire (LIF) model of a neuron. Taken together, these results suggest that even small changes in membrane properties or in tonic inputs that affect f_{DC} can have a substantial impact on the ability of a neuron to encode certain inputs with reliably timed spikes.

METHODS

Slowly adapting motoneurons (Aplysia)

Aplysia care, immobilization, and dissection were carried out with the use of procedures given by Church and Lloyd (1994). Slowly adapting motoneurons were identified in the dissociated, intact buccal ganglion based on size, location, and firing criteria. We used neurons that were not spontaneously active and that fired regularly (after an accommodation transient) in response to applied DC inputs. The ISI coefficient of variation [CV; mean (μ) of intervals divided by the SD of the intervals] in response to these DC injections was 0.05 ± 0.03. Experiments were performed in artificial seawater with 0.5 mM Ca^{2+} to minimize synaptic inputs from other neurons. Typical input resistances were ~5–10 MΩ.

Input signals

Periodic (sinusoidal) input signals were generated numerically with the use of an AD2210 (Real Time Devices) A/D board interfaced with a personal computer. A set of aperiodic input signals used in a single experiment was generated as follows. A white noise signal from an analog noise generator (model 1390-B, General Radio) was filtered with an analog low-pass Bessel filter (model 902, Frequency Devices) with a corner frequency of 2 kHz and was digitally sampled at 4 kHz. This noise was then convolved with an α-function, i.e., $f(t) = t \exp(-t/\tau)$, where $\tau = 4$ ms to create the broadband signal A. Signal A was then filtered with a Chebyshev type I band-stop digital filter with a band-stop region from 0.85 to 1.15 f_{DC} to create signal B. The same signal A was used to create the control signal C with a band-stop region from 0.4 to 0.7 f_{DC}. The digital filtering was performed with the use of the Matlab software package (The MathWorks). A different set of three signals was used for each experiment. These three signals were normalized so that the μ, SD, and rms amplitude (σ_s) were equal.

Stimulation protocol

The DC component of the current injections ranged from 5 to 22 nA, generating firing frequencies ranging from 7 to 24 Hz. This firing rate range encompasses the upper end of the physiological range at which most buccal neurons fire during feeding behavior (Church and Lloyd 1994). Slower firing rates were not examined because it was difficult to design notch filters for very low frequencies and to maintain the neuron in a stable state long enough to collect sufficient numbers of spikes for statistically reliable results. Recordings were performed in bridge mode with an AxoClamp 2B amplifier. All D/A and A/D signals were low-pass filtered with an analog Bessel filter (model 902, Frequency Devices) with a corner frequency of 2 kHz and were digitized at 4 kHz. The current stimulation protocol was automated, and cells were stimulated for 2 s with an interstimulus interval of 6–8 s, depending on the experiment. Cells were first stimulated with a series of DC inputs, and the average instantaneous firing frequency was computed over the second one-half of each stimulus interval; if the average rate was stable for two consecutive trials, the aperiodic stimulus protocol began with the use of precomputed input signals with the appropriate frequency content for this firing rate. This rate defined f_{DC} for the duration of the experiment. Ten blocks of the four stimuli (DC, A, B, and C) were presented; the presentation order within each block of four was randomized over the 10 trials.

Reliability statistic ($\mathcal{R}$)

To quantitatively evaluate spike timing reliability, we developed a reliability statistic. For each voltage trace, a corresponding point-process spike train record was determined (Perkel et al. 1967). A computationally efficient way to assess the extent to which N spike trains have spikes occurring at the same time is to add the point processes together and compute the time-series variance σ_x^2 of the sum, defined as

$$\sigma_x^2 = \frac{1}{t}\int_0^t x(\tau)^2 \mathrm{d}\tau - \left(\frac{1}{t}\int_0^t x(\tau)\mathrm{d}\tau\right)^2 \quad (1)$$

where x is constructed by summing the N separate point-process spike trains and t is the length of the record. If the spike times are completely independent in each of the N spike records, then each point in the summed record will contain on average the same number of spikes as any other point, and the time-series variance will approach zero with large N. On the other hand, if each of the M spike times are identical in each of the records, then the summed record will contain N spikes at each of the M times where a spike occurs and none otherwise. In this case the time-series variance will be maximal.

The formulation (*Eq. 1*), however, makes no distinction between two spikes that occur closely together (although not at the same time) and two spikes that are distant. Therefore we convolved the summed record with a weighting function that spreads the effect from the spikes temporally

$$X(t) = \int_0^t x(\tau)h(t-\tau)\mathrm{d}\tau \quad (2)$$

The time-series variance σ_X^2 of the weighted spike-train sum $X(t)$ is computed by substituting X for x into *Eq. 1*. We chose the weighting function

$$h(t) = \begin{cases} \lambda \exp^{-\lambda t} & \text{if} \quad t \geq 0 \\ 0 & \text{otherwise} \end{cases} \quad (3)$$

We normalized the reliability statistic $\mathcal{R}$ so that it ranged between zero and one by comparing it with the maximum value expected if each of the M spikes in the N spike trains occurred simultaneously. If the minimum interspike interval is long compared with λ^{-1}, the value σ_{max} (see APPENDIX) is

$$\sigma_{max} = \frac{N^2 M\lambda}{2t} - \frac{N^2 M^2}{t^2} \quad (4)$$

where t is the length of the record. The reliability statistic is then the time-series variance normalized so that it ranges from zero to one

$$\mathcal{R} = \sigma_X^2/\sigma_{max}^2 \quad (5)$$

Other statistics for spike time reliability were developed (see Victor and Purpura 1996 and references therein). The main advantage of our method is that it can be computed on a spike-by-spike basis in real time, and the use of adaptive smoothing filters (Mainen and Sejnowski 1995; Nowak et al. 1997) is not required. The correlation coefficient between our reliability statistic and that used in Mainen and Sejnowski (1995) for our data was $r = 0.96$.

Data analysis

We compared the reliability of spike timing in response with signals that contain frequencies around f_{DC} and in response to signals that do not. Because the *Aplysia* motoneurons accommodate, f_{DC} changes during the stimulus period. Thus statistics were computed over the region where the average instantaneous firing frequency in response to the DC component alone was within the band-stop region around f_{DC} defined by signal B. In addition we required that $\geq$70% of these spike trains fell within this interval. This requirement helps exclude those cases in which the firing rate of the neuron slowly changed from stimulation to stimulation. Experiments in which this interval was $<$0.5 s in length were discarded; 14 experiments failed to meet these criteria. For the 48 experiments that did satisfy the criteria, the length of the analysis interval was 1.3 $\pm$ 0.34 s.

The value $\lambda^{-1} = 10$ ms was used for the weighting function in *Eq. 3* because small differences in buccal motoneuron spike times on this scale were shown to have a dramatic effect on excitatory junction potentials in a facilitation paradigm (Cohen et al. 1978). Other choices of λ^{-1} over the range 2–10 ms changed the value of $\mathcal{R}$ for a given experiment but did not qualitatively alter the results.

Nonlinear regressions were performed (SigmaPlot) with the Marquardt-Levenberg algorithm (Press et al. 1992) with a double

exponential model function (see RESULTS). The use of linear or single-exponential model functions did not change the significance of the findings.

LIF model

The LIF neuron can be represented by an *RC* circuit with a current source and a potential reset after an action potential at threshold. The membrane potential between firings is given by the solution to

$$\frac{dV(t)}{dt} = -\frac{1}{RC}V(t) + \frac{1}{C}I(t) \tag{6}$$

where $V(t)$ is the membrane potential, R is the membrane resistance, C is the membrane capacitance, and $I(t)$ is the input current. The potential is reset to zero after an action potential at threshold θ; spikes with an amplitude of 100 mV are added at threshold crossings in the figures for ease of viewing.

For periodic inputs, $I(t) = \mu(1 + m \sin(2\pi ft + \phi)) + \sigma_n \xi(t) \sqrt{\Delta t}$ where μ is equal to the mean of the current, m is the fractional modulation amplitude, f is the frequency, ϕ is the phase, and $\xi(t)$ is the Gaussian distributed white noise with zero mean and unit variance. σ_n is a constant that scales the SD of the noise term. The step-size of numerical integration was $\Delta t = 0.5$ ms; this value was chosen because it is small compared with the membrane time constant over the parameters investigated, and the reliability statistic remained approximately constant with smaller step-size choices. The equation was integrated in FORTRAN with the use of a fourth-order Runge-Kutta algorithm *rk4*. The neuronal current noise was generated numerically with the use of pseudo-random number generator *gasdev* from Press et al. (1992), which is based on the Box-Muller algorithm.

The aperiodic inputs were generated as described above for the *Aplysia* inputs, and a noise term was added to simulate the intrinsic noise in the preparation. To assess spike timing reliability of the LIF model for aperiodic inputs, 20 phase-randomized surrogates each of signals A, B, and C were generated. Each surrogate input has the same power spectrum as the original but has a randomized phase spectrum (Theiler et al. 1992).

RESULTS

Periodic inputs

The effect of periodic stimulation on neurons that fire periodically was extensively studied both experimentally (Knight 1972b; Matsumoto et al. 1980; Perkel et al. 1964) and theoretically (Ascoli et al. 1977; Glass et al. 1980; Holden 1976; Keener et al. 1981; Knight 1972a; Rescigno et al. 1970; Scharstein 1979). For some modulation amplitudes and frequencies, it is possible for the neuron to become entrained to the periodic stimulus so that for each n cycles of the stimulus there are m cycles of the spontaneous rhythm (n:m phase locking). In addition to regular, phase-locked patterns of neuron firing, complex aperiodic firing patterns arise in some parameter regimes (Glass et al. 1980; Hayashi et al. 1983; Ishizuka and Hayashi 1996; Kaplan et al. 1996). The critical frequency f_{DC} plays a special role in neural phase-locking because 1:1 phase locking occurs even in the limit of vanishingly small modulation amplitude (Knight 1972a).

These studies did not specifically address the issue of spike time reliability as a function of input frequency. To illustrate the effects of the frequency, f, of a periodic input on the spike timing reliability, we stimulated an *Aplysia* buccal motoneuron with a periodic current of the form $\mu(1 + m \sin(2\pi ft))$. The mean spike frequency when the neuron was stimulated by the DC component alone was used to estimate f_{DC}. When $f/f_{DC} = 1.0$, a 1:1 phase locking pattern was observed, and when $f/f_{DC} = 0.65$, an irregular response pattern was obtained. Figure 2 shows the spike timing reliability for these two choices of f/f_{DC}. Clearly, spike timing reliability is much poorer when the input frequency is such that a simple phase-locking pattern does not arise (cf. Fig. 2*A* with 2*B*).

Aperiodic inputs

The observations shown in Figs. 1 and 2 suggest that aperiodic signals that contain the frequency band around f_{DC} will lead to more reliable spike times than signals lacking this component. To test this hypothesis, we constructed sets of three different aperiodic input signals: signal A consisted of broadband, low-pass filtered noise; signal B was constructed as signal A was, except that frequencies around and including f_{DC} were removed by digital filtering; and signal C was a control signal with a band removed below f_{DC}. Figure 3 shows a detail of one set of these three signals with their power spectra. In each case the signals have an identical μ, SD, and σ_s. Although the currents cannot be easily distinguished by visual inspection alone, they are readily distinguishable by their power spectra.

Figure 4 shows the results of a single trial in which signals A, B, C, and D were repeatedly presented to an *Aplysia* neuron. When a DC input is injected into the neuron, the spike timing between trials is least reliable ($\mathcal{R}_{DC} = 0.08$). When the broadband signal A containing f_{DC} is given to the neuron, the spike timing is most reliable ($\mathcal{R}_A = 0.54$). However, when the aperiodic signal B lacking f_{DC} is presented to the neuron, there is a substantial decrease in spike time reliability ($\mathcal{R}_B = 0.19$). Removing other frequency bands but leaving f_{DC} did not have a significant effect on spike timing reliability ($\mathcal{R}_C = 0.53$).

To examine the effect of the amplitude of the input current fluctuations on spike time reliability, it is necessary to normalize this amplitude to the magnitude of a current sufficient to cause neuronal spiking. This need arises, in part, because the neurons investigated varied in size. In our experiments, the magnitude of the DC component was chosen to trigger repetitive spiking in the physiological range (see METHODS), and thus this value, the mean of the current inputs, serves as an appropriate normalization factor. Thus we describe the amplitude fluctuations in the input current by the CV, i.e., the SD divided by the mean.

Figure 5 examines the enhancement of spike time reliability by frequency content around f_{DC} as a function of the CV of the input current. At each point, we plot the ratio of reliability generated by the band-stop signals ($\mathcal{R}_B$ or $\mathcal{R}_C$) to the reliability generated by the broadband signal ($\mathcal{R}_A$). If the band around f_{DC} is critically important, one expects the ratio $\mathcal{R}_B/\mathcal{R}_A < 1$ and the ratio $\mathcal{R}_C/\mathcal{R}_A \approx 1$ because in the former case only signal A contains the frequency band, whereas in the latter case both signals contain it. For modulation amplitudes that are small compared with the DC compo-

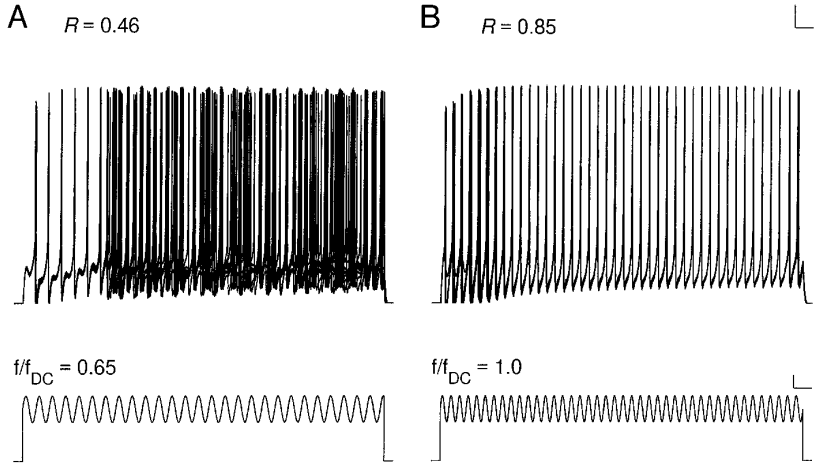

FIG. 2. Spike time reliability in *Aplysia* motoneurons with periodic inputs is dependent on f_{DC}. Superposed voltage traces from 10 different trials recorded from a buccal motoneuron for 2 different periodic current inputs: *A*: $f/f_{DC} = 0.65$; *B*: $f/f_{DC} = 1.0$, where f is the frequency of the periodic input, and f_{DC} is the firing rate in response to the DC component of the periodic input. $\mu = 20$ nA, $f_{DC} = 21$ Hz, and the amplitude is 5 nA. Scale bar for voltage traces is 10 mV by 100 ms and for current traces is 5 nA by 100 ms.

nent, this dependence on f_{DC} is pronounced and decreases with increasing modulation amplitude. When the CV is high, there is no effect on spike time reliability from filtering the aperiodic signals; all signals generate almost perfectly reliable firing times. Previous studies that showed highly reliable firing times utilized inputs in the large fluctuation amplitude limit [$\sigma_s/\mu = 0.67$, as shown in Fig. 1 of Mainen and Sejnowski (1995)].

To statistically quantify this effect, we fit the experimental data to the model function $y(x) = 1 + e^{-\alpha x} - e^{-\beta x}$, where x is the input current CV and y is the mean ratio of the reliabilities generated by two signals to be compared (Fig. 5). This model function was chosen because it is constrained to be one at $x = 0$, which must be the theoretical value because the two signals will be the same at zero modulation amplitude and will also equal one for sufficiently large values of x. The second condition arises because it is presumed that either input signal will generate highly reliable firing times at sufficiently large fluctuation amplitudes [as was observed in Mainen and Sejnowski (1995)], and thus the $\mathcal{R}$ ratio will be one. The decay constants of the two exponentials for the function plotted in Fig. 5*A* are $\alpha = 22.5$ and $\beta = 7.4$ and in Fig. 5*B* are $\alpha = 6.8$ and $\beta = 5.9$. This analysis (see Fig. 5 legend) indicates that aperiodic signals lacking the frequency band around f_{DC} generate significantly less reliably timed spikes than either the broadband signal or the control band-stop signal. Moreover, this dependence

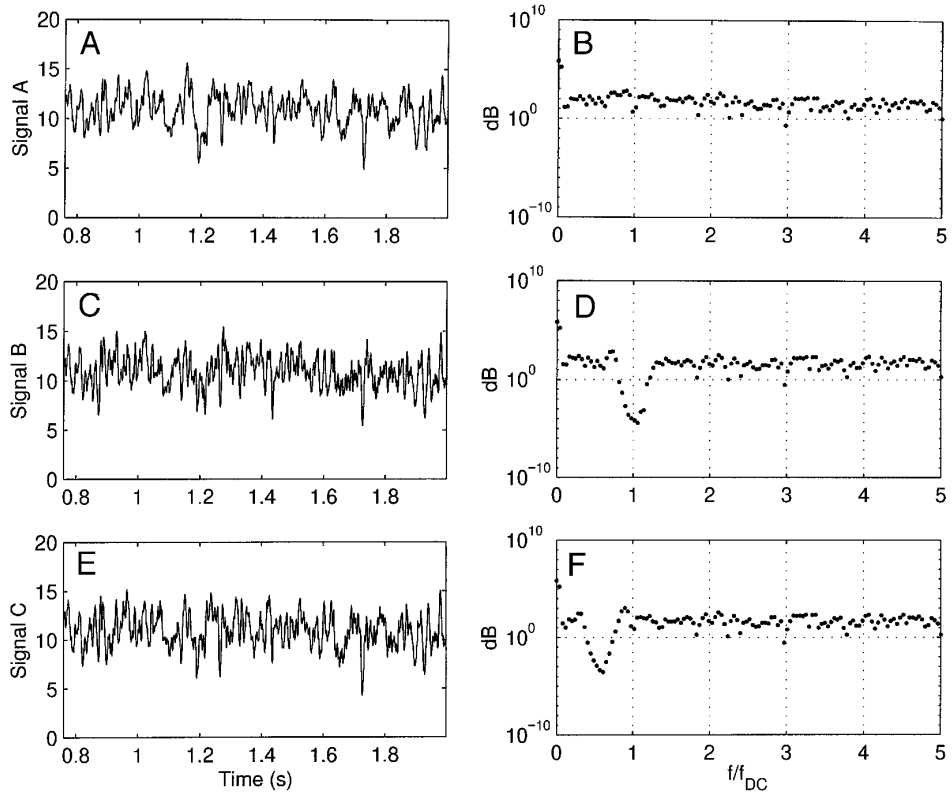

FIG. 3. A detail of 3 current traces (*A*, *C*, and *E*) with their power spectra (*B*, *D*, and *F*). *Top panels*: broadband signal A. *Middle panels*: signal B with a band-stop region around the critical frequency f_{DC}. *Bottom panels*: signal C, which is a control signal with a band-stop region below and does not include f_{DC}. $\mu = 10.9$ nA, $\sigma_s = 1.6$ nA. Power spectra shown were computed with Welch's average periodogram method from a long segment of the three signals; the traces used in the adjacent plots are samples from this longer segment. Current traces (*A*, *C*, and *E*) show in greater detail the regions between the hatch marks and the end of the current step in Fig. 4.

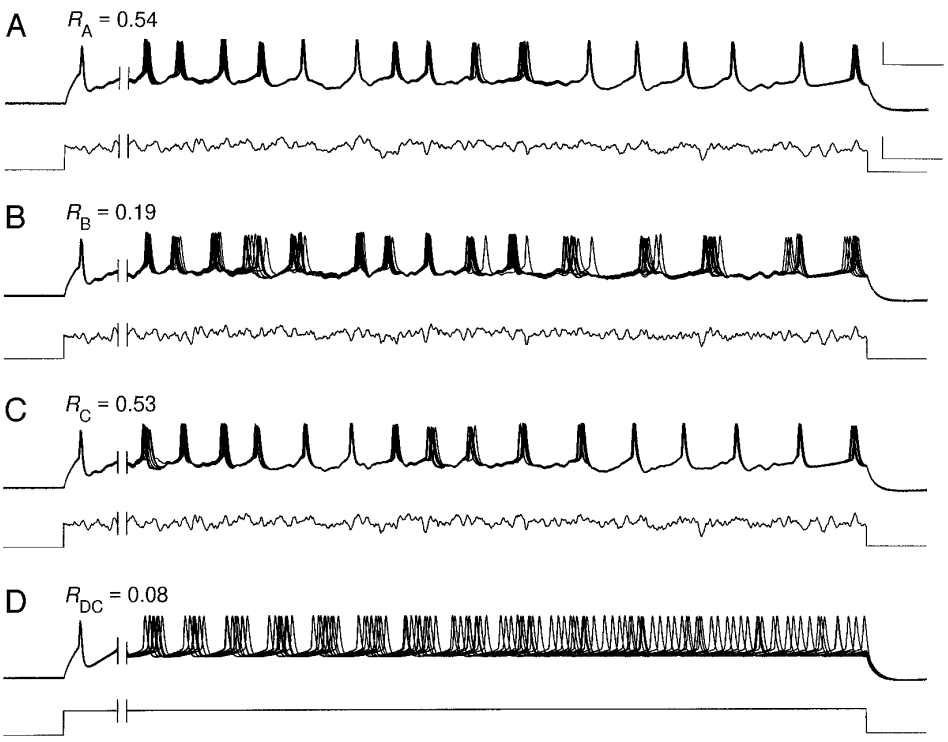

FIG. 4. Spike time reliability in *Aplysia* motoneuron with aperiodic inputs. Superposed voltage traces from 10 different trials recorded from a buccal motoneuron for 4 different input signals. *A*: broadband aperiodic input; *B*: band-stop input lacking frequencies around f_{DC}; *C*: band-stop control input lacking frequencies ~0.55 f_{DC} but containing frequencies around f_{DC}; *D*: DC component only. Current input signals are shown underneath the spike trains (signals *A*–*D*, respectively); the region between the hatch marks and the end of the signal may be seen in greater detail in Fig. 3. All traces shown here (*A*–*D*) are from a single experiment in which the order of the 40 current presentations was randomized; the means and SDs of the aperiodic current inputs are equal; $\mu = 10.9$ nA, $\sigma_s = 1.6$ nA. Although all aperiodic input signals (*A*–*C*) generated more reliable firing times than did the DC trial, signals containing power in the frequency bands around f_{DC} (*A* and *C*) generated significantly more reliable firing times than those that did not (*B* and *D*); see Fig. 5. Spike time reliability for each series is given above each voltage trace. Hatch marks denote a region of 0.68 s in length that is not plotted because the neuron is accommodating and the firing frequency is outside the analysis region. Scale bar above voltage trace in *A* is 20 mV by 100 ms and above current trace is 10 nA by 100 ms; axes in *B*–*D* are scaled similarly.

is a function of the relative amplitude of the current fluctuations.

Integrate-and-fire model

The spike timing reliability of a LIF model of a neuron was examined for the same type of inputs used to stimulate the *Aplysia* motoneuron. We choose to study a LIF model because this is the simplest representation that incorporates two essential properties of a spiking neuron, i.e., a firing threshold and leaky integration. For this model (*Eq. 6*), the critical frequency f_{DC} is

$$f_{DC} = -\frac{1}{RC}\left[\ln\left(1 - \frac{\theta}{\mu R}\right)\right]^{-1} \tag{7}$$

where μ is the DC input current. The observation that spike

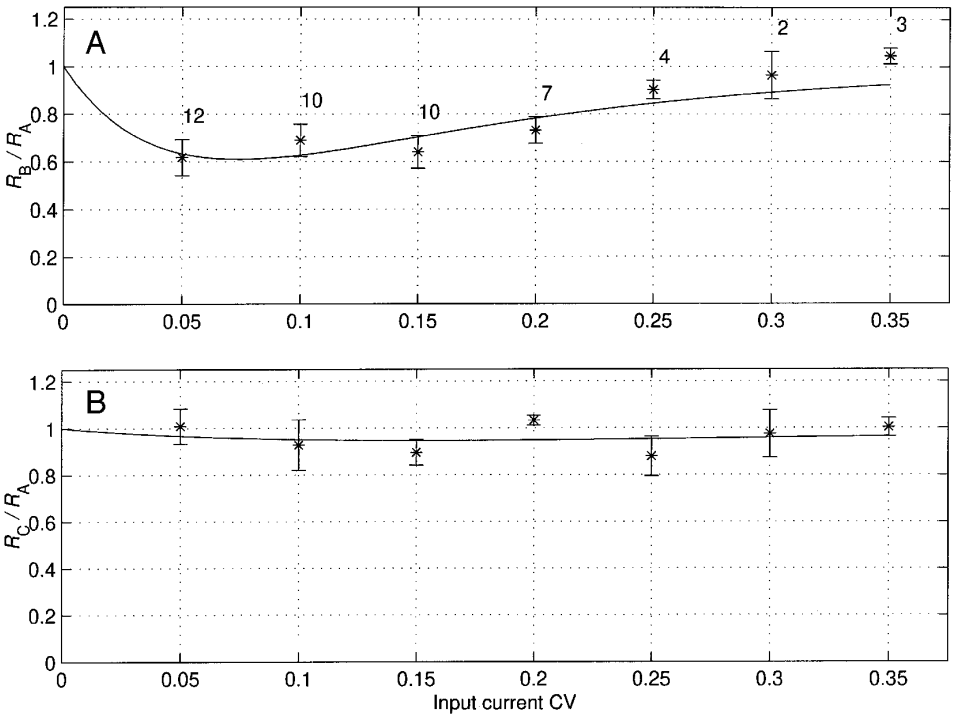

FIG. 5. Dependence on f_{DC} for aperiodic inputs is a function of input current coefficient of variance (CV). Spike time reliability for each input was computed from the firing times in 10 trials. The mean and standard error of the ratio of the reliability generated by a band-stop signal ($\mathcal{R}_B$ or $\mathcal{R}_C$) to that generated by a broadband signal ($\mathcal{R}_A$) is plotted for each CV value. Some experiments had CV values that did not fall along the abscissa points plotted; in those cases the nearest CV value was chosen. The number of experiments used in computing each point is shown above the error bars in *A*. An experiment where a band-stop and a broadband signal generate equally reliable firing times will fall along the horizontal line at one. Statistics cited are from a nonlinear regression, and the solid lines show the best fit to a double-exponential model function. *A*: band-stop removes a frequency band around and including f_{DC} ($F_{(1,46)} = 10.9$, $P < 0.002$). *B*: band-stop removes a frequency band below and not containing f_{DC} ($F_{(1,46)} = 0.8$, nonsignificant). A different set of aperiodic signals was used in each experiment. The data presented in Fig. 4 fall at 0.15 on the abscissa.

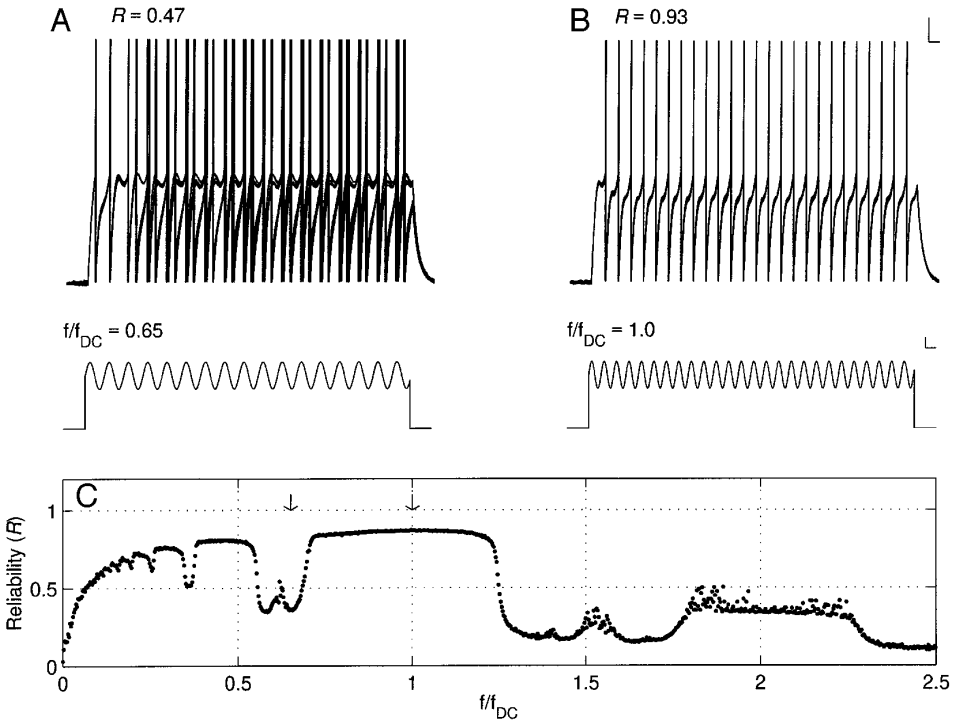

FIG. 6. Spike timing reliability for the leaky integrate and fire model (LIF) of a neuron with periodic inputs. Top panels show superposed voltage traces from 40 presentations of periodic input to the model at (*A*) $f/f_{DC} = 0.65$ and (*B*) $f/f_{DC} = 1.0$. Current traces are shown below. Scale bar for voltage traces is 10 mV by 100 ms and for current traces is 2 nA by 100 ms. Results for a range of frequencies are summarized in *C*. Each point indicates the spike time reliability in response to a single frequency input, repeatedly presented (40 times for 15 s each) to a model neuron with an independent white noise current. Reliable spike times are observed at harmonics and subharmonics of f_{DC}. Arrows indicate the frequencies $0.65\,f_{DC}$ and $1.0\,f_{DC}$ from the *Aplysia* experiments and simulations shown in *A* and *B* of Figs. 1, 2, and 6. $\mu = 10$ nA, $m = 0.25$, $R = 5$ MΩ, $C = 10$ nF, $\theta = 45$ mV, $f_{DC} = 8.7$ Hz, $\sigma_n = 40$ nA.

times in response to DC inputs are unreliable implies that there is some intrinsic noise in the current source (Calvin and Stevens 1968; Fatt and Katz 1950; Mainen and Sejnowski 1995; Tuckwell 1989). To incorporate this feature, we added a small amount of Gaussian distributed white noise to the current source in the model.

The reliability of the LIF model for periodic inputs is shown in Fig. 6. As was observed in *Aplysia*, periodic inputs at the critical frequency generated highly reliable firing times in the presence of noise, in contrast to nearby frequencies (cf. Fig. 6*A* with 6*B*). Two parameters in the model were matched with those of the *Aplysia* experiment presented in Fig. 2, the ratio f/f_{DC} and fractional modulation amplitude m. Figure 6*C* shows the reliability summarized for a broad range of frequencies. Maximal spike time reliability occurs around $f/f_{DC} = 1.0$. Enhanced reliability is also seen in peaks around the harmonics and subharmonics of f_{DC}. This was also observed for the *Aplysia* motoneurons (not shown). For other frequencies, such as $f/f_{DC} = 0.65$, the reliability is poor. The qualitative features of Fig. 6C can be readily understood by examining fixed points of the firing time return map for the LIF model with periodic inputs (Rescigno et al. 1970); the sharp transitions from highly reliable firing times to low reliability correspond to the loss of stable fixed points in the return map.

A full treatment of the parameter space of the LIF model with periodic inputs in the absence of noise is given by Keener et al. (1981). Bulsara et al. (1996) made progress on the stochastic model under the assumptions that $\theta/\mu R \approx 1$ and that the period of the forcing is the slowest time scale in the system. Our work shows that extensions of the model to include refractory periods and nonlinear conductance terms preserve the features of Fig. 6*C*. Although these additions significantly affect the value f_{DC}, the locations of the peaks remain around the harmonics and subharmonics of f_{DC} (not shown).

The spike timing reliability of the LIF model to aperiodic inputs is summarized in Fig. 7. We presented broadband signals A and band-stop signals B and C to the model and computed the reliability of spike times in the presence of noise. For all aperiodic signals, reliability increased with the input current CV, and the form of this increase parallels that demonstrated by Mainen and Sejnowski (1995). This is expected from slope arguments (cf. Fig. 1). Figure 7 shows the reliability for the three signals A, B, and C as a function of input current CV. Although reliabilities of all three increased with input current CV, the band-stop signal B (asterisks), lacking the frequency band around f_{DC}, generated appreciably less reliable spike time responses than did the broadband signal A and the control band-stop signal C. An additional control signal with a band-stop region above f_{DC} was also investigated. This signal, like the control signal C, did not generate significantly different reliability statistics from signal A (not shown). Thus only the aperiodic signals lacking the frequency band f_{DC} generated significantly less reliable spike trains in the presence of noise.

This difference is illustrated by comparing the ratio of the reliability in response to the band-stop with that in response to the broadband signal (Fig. 8, *A* and *B*) for the model. We plotted ±SD bars about the mean of the ratio of the reliability statistics for the 20 sets of signals tested at each point, so the mean (not plotted) will fall at the midpoint of these bars for any point along the abscissa. For modulation amplitudes small compared with the intrinsic noise source (SD of noise/mean of controlled input equals 0.09), the system is dominated by the noise, and there is a large deviation about one,

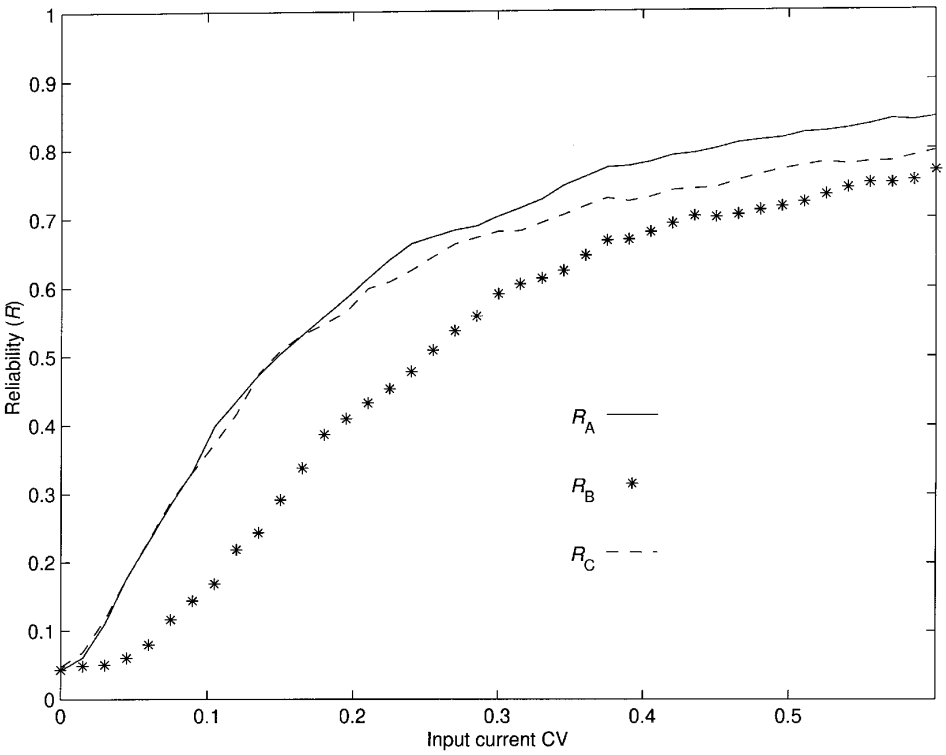

FIG. 7. Spike timing reliability for the LIF model of a neuron with aperiodic inputs. The three aperiodic signals A, B, and C were presented (40 times for 8.2 s each) to the LIF model in the presence of noise, and the spike time reliability $\mathcal{R}$ was computed. This procedure was repeated for 20 different sets of signals A, B, and C and the average response at each input current CV is shown. Signal A, solid line; signal B, asterisks; signal C, dashed line. Only signal B lacks the band around the critical frequency f_{DC}. Model parameters are the same as those in Fig. 6.

indicating that the reliability was dictated by chance rather than the controlled input.

As the modulation amplitude of the controlled input approaches that of the intrinsic noise level, one begins to see an effect of the frequency content of the input signal on spike time reliability. For the band-stop signal B, lacking the frequency band around f_{DC}, there is more than a twofold decrease in the spike time reliability when compared with the broadband signal A for input current CVs around 0.05–0.12 (Fig. 8*A*). The effect decreases with increasing modulation amplitude (see DISCUSSION). For the control signal C, both signals contain the frequency band around f_{DC}. Thus

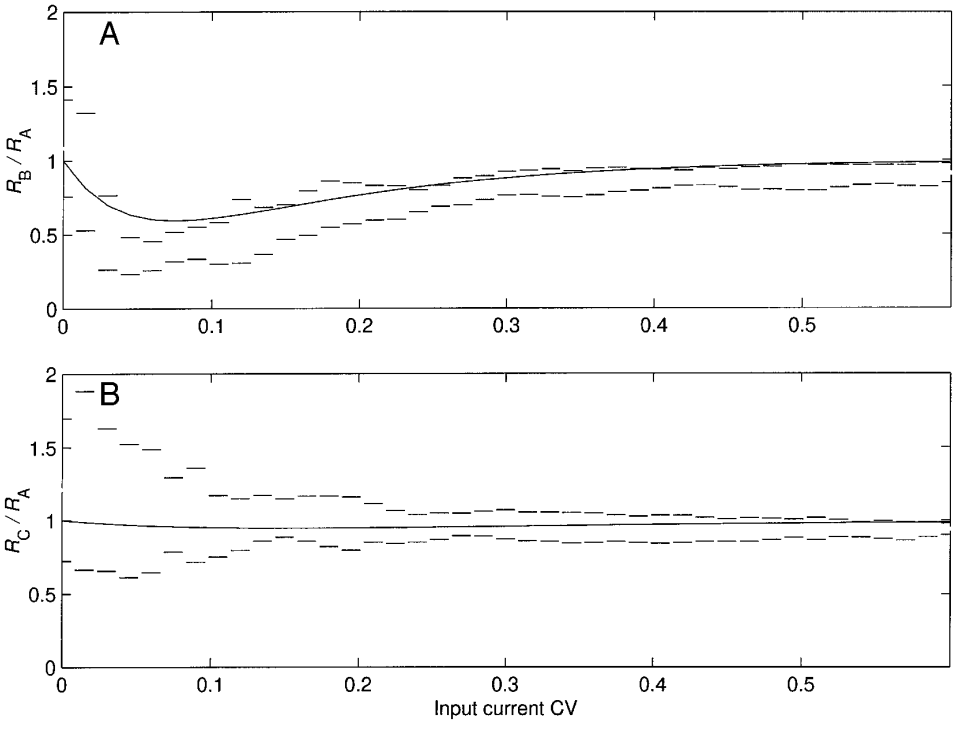

FIG. 8. Dependence on critical frequency for aperiodic inputs to leaky integrate and fire model is a function of input current CV. *A*: average ratio of $\mathcal{R}_B/\mathcal{R}_A$ is computed as a function of current CV. A ratio of one indicates no effect from filtering the signal on spike time reliability. Bars show the mean ± SD of the reliability ratio from 20 different sets of signals A, B, and C at each point. *B*: ratio of $\mathcal{R}_C/\mathcal{R}_A$ is plotted. The best fit curves from the *Aplysia* data presented in Fig. 5 are plotted with solid lines for comparison. Ratios are computed from the same data presented in Fig. 7.

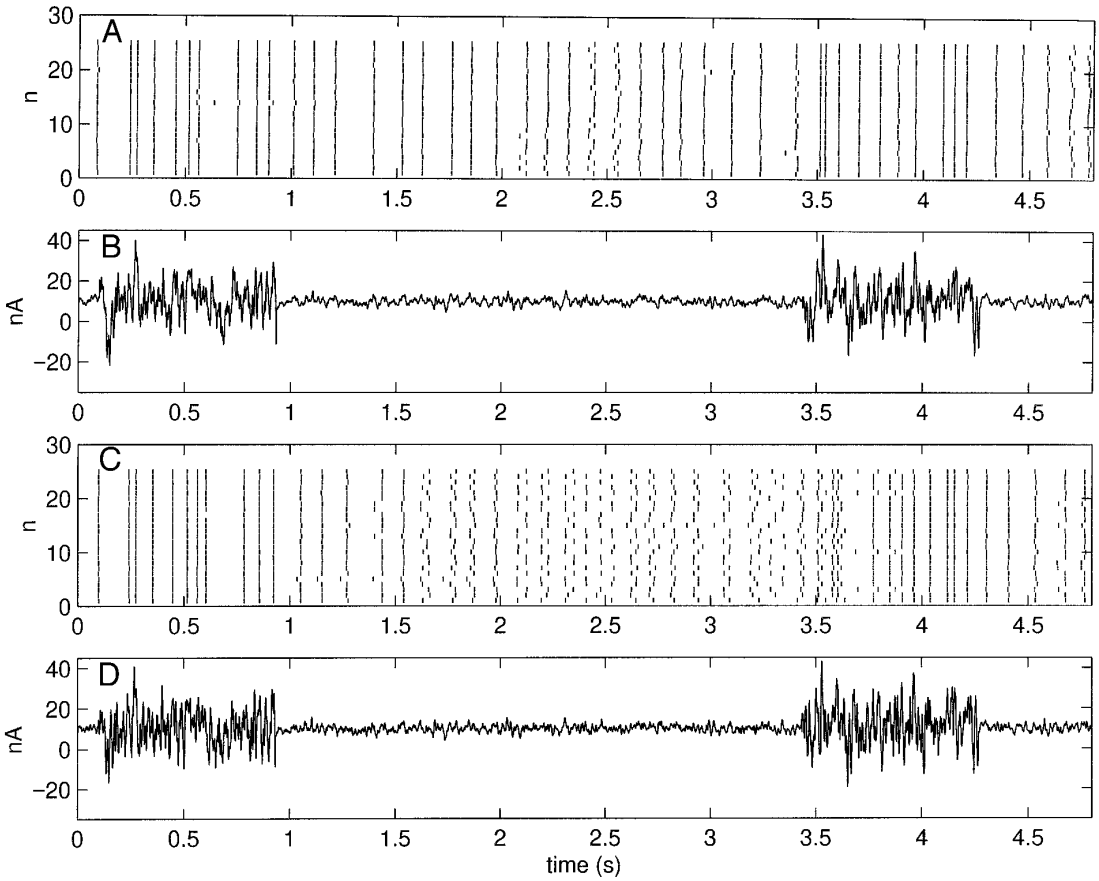

FIG. 9. Spike time reliability as a function of the magnitude of current fluctuations for the LIF model receiving (*B*) a broadband current input A and (*D*) a band-stop current input B lacking frequencies around f_{DC}. Modulation intensity of these currents was periodically increased to mimic situations where neurons receive bursts of large amplitude inputs, as in regularly spiking cortical neurons during sleep. During the burst periods, the amplitude of the input current fluctuations is high (CV = 1) and spike timing reliability is insensitive to the presence of f_{DC} (cf. raster plots in *A* and *C*). In the regions between the bursts, where the amplitude of the current fluctuations is small (CV = 0.15), spike timing reliability is sensitive to the presence of f_{DC} (compare raster plots in *A* and *C*). Parameters for the LIF model are the same as in Fig. 6.

the mean of the ratio $\mathcal{R}_C/\mathcal{R}_A \approx 1$ at all modulation amplitudes, indicating no effect of filtering on spike time reliability (Fig. 8*B*). In Fig. 8, *A* and *B*, the solid line shows the best fit line to the *Aplysia* data for comparison with the model. The line for the experimental data falls within ~1 SD of the mean of the model results.

DISCUSSION

The relevance of our observations for spike time reliability is illustrated schematically in Fig. 9. The amplitude of the input signal to a neuron typically shows considerable variation, with regions of small fluctuations interspersed with large fluctuations. Examples include regularly spiking cortical neurons undergoing sleep rhythms (Steriade et al. 1993), *Aplysia* motor neurons during feeding like behavior (Church and Lloyd 1994), evoked responses of visual cortical neurons (Jagadeesh et al. 1992), and spiny neostriatal neurons receiving synaptic barrages (Wilson and Kawaguchi 1996). When the amplitude of the fluctuating component is large enough alone to cause a neuron to spike (burst regions in Fig. 9, *B* and *D*), spike timing will be reliable (Fig. 9, *A* and *C*). However, the spike time reliability that occurs under these conditions is insensitive to the frequency content of the input (cf. Fig. 9*A* with 9*C*). Our results indicate that, even when the amplitude of the fluctuations is small (interburst regions of Fig. 9, *B* and *D*), it is possible for spike timing to be reliable. In contrast, for small amplitude fluctuations spike timing reliability is sensitive to the frequency content of the input (cf. Fig. 9*A* with 9*C*). This is because under these considerations the mechanism for spike timing reliability operates through a resonance phenomenon. Thus information stored in small fluctuations in a neuron's input can also be transmitted in the form of reliable spike times. That the same results were observed whether we studied *Aplysia* motoneurons or an integrate and fire neuron suggests that they are a general property of encoders that combine a threshold with a leaky integrator (Knight 1972a).

The resonance-related enhancement in spike time reliability is greatest when the amplitude of the input current fluctuations is small. An analysis of the effect of the amplitude of current fluctuations on spike time reliability must take into account the size of the neuron because larger currents are needed to stimulate larger neurons to fire. With this in mind we normalized the magnitude of the fluctuations in the input current to the magnitude sufficient to cause neuronal

spiking (expressed as the CV). The resonance-related enhancement in spike time reliability is maximal when CV ~0.05–0.15. However, other normalizations would serve equally well and may be more experimentally accessible than current magnitudes. For example, one such approach utilizes the ISI distribution resulting from the aperiodic input current. The definition of small in the requirement of small modulation amplitude essentially requires that the spike intervals generated by the aperiodic current approximate T_{DC}. Thus the mean and width of the ISI distribution generated by the aperiodic input currents serve as a measure for the importance of the contribution of f_{DC} to the current spectrum. The expectation is that distributions with means far from T_{DC} or broad widths will not show the f_{DC} dependence. We also examined the reliability ratios from Fig. 5 as a function of the CV of the ISI distribution generated by the application of the broadband signal A. With qualitatively similar results, the maximal effect was found for interval CVs ranging from 0.15 to 0.25.

The resonance phenomena that give rise to reliable spike times when the fluctuations are small are intimately dependent on the interplay between the frequency content of the input current fluctuations and the neuron's firing rate, f_{DC}. For example, we observed a twofold decrement in spike timing reliability in signals with a band-stop ~14 Hz (B) compared with signals with a band-stop ~10 Hz (C) for small-amplitude signals. The frequency f_{DC} encapsulates many parameters of the neuron, including the action potential threshold, leakiness of the membrane, and afterhyperpolarizing currents (Baldissera and Gustafsson 1971; Kernell 1968; Schwindt and Calvin 1972; Stein 1967a). Modifications in any of these parameters that bring the firing rate into the range where the frequency spectrum of the current fluctuations contains power may switch the neuron from a mode where only the rate is reliable to one where the times are reliable as well. Conversely, modifications that affect the frequency spectrum, such as changes in the time courses of synaptic currents, can have the same effect.

A recent study also examined the relation between spike time reliability and the frequency content of an aperiodic input to a neuron (Nowak et al. 1997). These authors showed that large amplitude, high-frequency inputs in the γ range (30–70 Hz) facilitate spike time reliability compared with a low-frequency input. Because the two signals used by these authors had different SDs, it is not possible to ascribe the observations solely to the spectral content of the input. Nonetheless, high-frequency fluctuations such as those in the γ range would be expected to increase the slope of the membrane potential at threshold crossings, thus leading to increased spike time reliability. The role of γ range frequencies for small modulation amplitudes was not examined by Nowak et al. (1997). Our results suggest that for small-modulation amplitudes it is not the presence of γ range frequencies per se that facilitates spike timing reliability but the presence of frequencies around the spiking rate of the neuron (and possibly certain harmonics or subharmonics; see Fig. 6).

Although we discussed our results in terms of spike timing reliability for a single neuron, they are applicable to the synchronization of populations of uncoupled neurons to a coherent input. Such populations received attention because of their ability to encode subthreshold aperiodic inputs (Collins et al. 1995) and to recover the precise spike times of a coherent spike train input (Pei et al. 1996). Periodic inputs that cause stable $1:m$ phase locking, i.e., synchronization, are precisely those that generate reliable firing times in the presence of noise ($n:m$ phase-locked solutions where $n \neq 1$ generate less reliable spike times because there are multiple spike time solutions for a given cycle of input). Likewise, the synchronization of uncoupled populations to aperiodic inputs will have the same dependence on f_{DC} as was presented here in the context of spike time reliability.

Although our experiments do not address the question of whether precise spike times carry information in vivo, they do indicate necessary conditions for certain input signals to be reliably encoded with precise spike times. Not surprisingly, spike time reliability depends on both the intrinsic properties of the neuron as well as the nature of the input signal. What is surprising is the fact that there is a range of input modulation amplitudes for which small modifications in either the frequency content of the input or the firing rate of the neuron can dramatically alter spike timing reliability. That the same neuron can be either a rate or a spike time encoder may have important implications for neural coding.

APPENDIX

Here we determine the normalization factor σ_{max}. We assume that the number of spikes M is the same for each of the N spike trains. If the minimum ISI is long compared with λ^{-1}, then only the most recent spike from each spike train will make an appreciable contribution at time τ to the convolution integral in *Eq. 2*. Under this assumption, the time-series variance σ_X^2 is closely approximated by

$$\sigma_X^2 = \frac{1}{t}\int_0^t \left(\sum_{j=1}^{N} h(\tau - t_{ji})\right)^2 d\tau - \left(\frac{1}{t}\int_0^t \sum_{j=1}^{N} h(\tau - t_{ji}) d\tau\right)^2 \quad (8)$$

where t_{ji} is the most recent spike of the jth spike train at or before a given time τ.

To compute σ_{max}, we assume that each of the M spike times in the N records is identical. Letting $t_{ki} = t_{ji} = t_i$ for each of the $i = 1, \ldots, M$ spikes, and defining $t_0 = 0$ and $t_{M+1} = t$, one obtains on substitution of the exponential weighting function into *Eq. 8*

$$\sigma_{max}^2 = \frac{1}{t}\sum_{i=0}^{M}\int_{t_i}^{t_{i+1}} N^2\lambda^2 e^{-2\lambda(\tau - t_i)} d\tau - \left(\frac{1}{t}\sum_{i=0}^{M}\int_{t_i}^{t_{i+1}} N\lambda e^{-\lambda(\tau - t_i)} d\tau\right)^2 \quad (9)$$

Making the substitution $u = \tau - t_i$, and replacing the upper limits of integration with ∞ (because $t_{i+1} - t_i \gg \lambda^{-1}$ by assumption), the above expression is closely approximated by

$$\sigma_{max}^2 = \frac{N^2 M\lambda}{2t} - \frac{N^2 M^2}{t^2} \quad (10)$$

This is the expression given in *Eq. 4*.

We thank L. Fox and P. Lloyd for advice concerning *Aplysia* and assistance in the dissections. We also thank E. Curiel, A. Dimitrov, J. Foss, T. Mundel, and P. Ulinski for useful comments; J. Crate and B. Mintzer for assistance in the design of the electronics for these experiments and the computer hardware interfacing; and F. Moss for the donation of the noise generator.

This research was supported by grants from the National Institutes of

Mental Health and the Brain Research Foundation. J. D. Hunter was supported by a scholarship from the National Science Foundation.

Address for reprint requests: J. G. Milton, Dept. of Neurology, MC 2030, The University of Chicago, 5841 South Maryland Ave., Chicago, IL 60637.

Received 11 September 1997; accepted in final form 8 June 1998.

REFERENCES

ARIELI, A., STERKIN, A. GRINVALD, A., AND A. AERSTEN, A. Dynamics of ongoing activity: explanation of the large variability in evoked cortical responses. *Science* 273: 1868–1871, 1996.

ASCOLI, C., BARBI, M., CHILLEMI, S., AND PETRACCHI, D. Phase-locked responses in the *Limulus* lateral eye. *Biophys. J.* 19: 219–240, 1977.

BALDISSERA, F. AND GUSTAFSSON, B. Regulation of repetitive firing in motoneurones by the afterhyperpolarization conductance. *Brain Res.* 25: 431–434, 1971.

BULSARA, A. R., ELSTON, T. C., LOWEN, S. B., AND LINDENBERG, K., Cooperative behavior in periodically driven noisy integrate-fire models of neuronal dynamics. *Phys. Rev. E* 53: 3958–3969, 1996.

CALVIN, W. AND STEVENS, C. Synaptic noise and other sources of randomness in motoneuron interspike intervals. *J. Neurophysiol.* 31: 574–587, 1968.

CHURCH, P. J. AND LLOYD, P. E. Activity of multiple identified motor neurons recorded intracellularly during evoked feeding like motor programs in *Aplysia*. *J. Neurophysiol.* 72: 1794–1809, 1994.

COHEN, J. L., WEISS, K. R., AND KUPFERMANN, I. Motor control of buccal muscles in *Aplysia*. *J. Neurophysiol.* 41: 157–181, 1978.

COLLINS, J. J., CHOW, C. C., AND IMHOFF, T. T. Stochastic resonance without tuning. *Nature* 376: 236–238, 1995.

CRONER, L. J., PURPURA, K., AND KAPLAN, E. Response variability in retinal ganglion cells of primates. *Proc. Nat. Acad. Sci. USA* 90: 8128–8130, 1993.

FATT, P. AND KATZ, B. Some observations on biological noise. *Nature* 166: 597–598, 1950.

GEISLER, C. D. AND GOLDBERG, J. M. A stochastic model for the repetitive activity of neurons. *Biophys. J.* 6: 53–69, 1966.

GEISLER, W. S., ALBRECHT, D. S., SALVI, R. J., AND SAUNDERS, S. S. Discrimination performance of single neurons: rate and temporal pattern information. *J. Neurophysiol.* 66: 334–362, 1991.

GERSTNER, W., VAN HEMMEN, J. L., AND COWAN, J. D. What matters in neuronal locking? *Neural Comput.* 8: 1653–1676, 1996.

GLASS, L., GRAVES, C., PETRILLO, G. A., AND MACKEY, M. C. Unstable dynamics of a periodically driven oscillator in the presence of noise. *J. Theor. Biol.* 86: 455–473, 1980.

GOLDBERG, J., SMITH, C. E., AND FERNÁNDEZ, C. Relation between discharge regularity and responses to externally applied galvanic currents in vestibular nerve afferents of the squirrel monkey. *J. Neurophysiol.* 51: 1236–1256, 1984.

GUR, M., BEYLIN, A., AND SNODDERLY, D. M. Response variability of neurons in primary visual cortex (V1) of alert monkeys. *J. Neurosci.* 17: 2914–2920, 1997.

HAYASHI, H., NAKAO, M., AND HIRAKAWA, K. Entrained, harmonic, quasi-periodic and chaotic responses of the self-sustained oscillation of Nitella to sinusoidal stimulation. *J. Physiol. Soc. Jpn.* 52: 344–351, 1983.

HOLDEN, A. V. The response of excitable membrane models to a cyclic input. *Biol. Cybern.* 21: 1–7, 1976.

HOLT, G. R., SOFTKY, W. R., KOCH, C., AND DOUGLAS, R. J. Comparison of discharge variability in vitro and in vivo in cat visual cortex neurons. *J. Neurophysiol.* 75: 1806–1814, 1996.

HOPFIELD, J. J. Pattern recognition computation using action potential timing for stimulus representation. *Nature* 376: 33–36, 1995.

ISHIZUKA, S. AND HAYASHI, H. Chaotic and phase-locked responses of the somatosensory cortex to a periodic medial lemniscus stimulation in the anesthetized rat. *Brain Res.* 723: 46–60, 1996.

JAGADEESH, B., GRAY, C. M., AND FERSTER, D. Visually evoked oscillations of membrane potential in cells of cat visual cortex. *Science* 257: 552–554, 1992.

KAPLAN, D. T., CLAY, J. R., MANNING, T., GLASS, L., GUEVARA, M. R., AND SHRIER, A., Subthreshold dynamics in periodically stimulated squid giant axons. *Phys. Rev. Lett.* 76: 4074–4077, 1996.

KEENER, J., HOPPENSTEADT, F., AND RINZEL, J. Integrate-and-fire models of nerve membrane response to oscillatory input. *SIAM J. Appl. Math.* 41: 503–517, 1981.

KERNELL, D. The repetitive impulse discharge of a simple neurone model compared to that of spinal motoneurones. *Brain Res.* 11: 685–687, 1968.

KNIGHT, B. K. Dynamics of encoding in a population of neurons. *J. Gen. Physiol.* 59: 734–766, 1972a.

KNIGHT, B. K. The relationship between the firing rate of a single neuron and the level of activity in a population of neurons. Experimental evidence for resonant enhancement in the population response. *J. Gen. Physiol.* 59: 767–778, 1972b.

MAINEN, Z. F. AND SEJNOWSKI, T. J. Reliability of spike timing in neocortical neurons. *Science* 268: 1503–1506, 1995.

MATSUMOTO, G., KYUNG-SHIK, K., TAKESHI, U., AND SHIMADA, J. Electrical and computer stimulation upon the nervous activities of squid giant axons and around the state of spontaneous repetitive firing of action potentials. *J. Phys. Soc. Jpn.* 49: 906–914, 1980.

MIDDLEBROOKS, J. C., CLOCK, A. E., AND GREEN, D. M. A panoramic code for sound location. *Science* 264: 842–844, 1994.

NOWAK, L. G., SANCHEZ-VIVES, M. V., AND MCCORMICK, D. A. Influence of low and high frequency inputs on spike timing in visual cortical neurons. *Cereb. Cortex* 7: 487–501, 1997.

OPTICAN, L. M. AND RICHMOND, B. J. Temporal encoding of two-dimensional patterns by single units in primate inferior temporal cortex. III. Information theoretic analysis. *J. Neurophysiol.* 57: 162–178, 1987.

OTMAKHOV, N., SHIRKE, A. M., AND MALINOW, R. Measuring the impact of probabilistic transmission on neuronal output. *Neuron* 10: 1101–1111, 1993.

PEI, X., WILKENS, L., AND MOSS, F. Noise-mediated spike timing from aperiodic stimulus in an array of Hodgkin-Huxley-type neurons. *Phys. Rev. Lett.* 71: 4679–4682, 1996.

PERKEL, D. H. AND BULLOCK, T. H. Neural coding: A report based on an NRP session. *Neurosci. Res. Program Bull.* 6: 221–348, 1968.

PERKEL, D. H., GERSTEIN, G. L., AND MOORE, G. P. Neuronal spike trains and stochastic point processes. I. The single spike train. *Biophys. J.* 7: 391–418, 1967.

PERKEL, D. H., SCHULMAN, J. H., BULLOCK, T. H., MOORE, G. P., AND SEGUNDO, J. P. Pacemaker neurons: effects of regularly spaced synaptic input. *Science* 145: 61–63, 1964.

PRESS, W. H., TEUKOLSKY, S. A., VETTERLING, W. T., AND FLANNERY, B. P. Numerical Recipes in FORTRAN: The Art of Scientific Computing. Cambridge, 1992.

REDMAN, S., LAMPARD, D., AND ANNAL, P. Monosynaptic stochastic stimulation of cat spinal motoneurons II. Frequency transfer characteristics of tonically discharging motoneurons. *J. Neurophysiol.* 31: 499–508, 1968.

RESCIGNO, A., STEIN, R., PURPLE, R., AND POPPELE, R. A neuronal model for the discharge patterns produced by cyclic inputs. *Bull. Math. Biophys.* 32: 337–353, 1970.

DE RUYTER VAN STEVENINCK, R. R., LEWEN, G. D., S. P. STRONG, S. P., KOBERLE, R., AND BIALEK, W. Reproducibility and variability in neuronal spike trains. *Science* 275: 1805–1808, 1997.

SANDERSON, A., KOZAK, W., AND CALVERT, T. Distribution coding in the visual pathway. *Biophys. J.* 13: 218–244, 1973.

SCHARSTEIN, H. Input-output relations of the leaky-integrator neuron model. *J. Math. Biol.* 8: 403–420, 1979.

SCHWINDT, P. C. AND CALVIN, W. H. Membrane-potential trajectories between spikes underlying motoneuron firing rates. *J. Neurophysiol.* 35: 311–325, 1972.

SEGUNDO, J. P., PERKEL, D. H., AND MOORE, G. P. Spike probability in neurones: Influence of temporal structure in the train of synaptic events. *Kybernetik* 3: 67–82, 1966.

SOFTKY, W. R. Simple codes versus efficient codes. *Curr. Opin. Neurobiol.* 5: 239–247, 1995.

SOFTKY, W. R. AND KOCH, C. The highly irregular firing of cortical cells is inconsistent with temporal integration of random EPSPs. *J. Neurosci.* 131: 334–350, 1993.

STEIN, R. B. A theoretical analysis of neuronal variability. *Biophys. J.* 5: 173–194, 1965.

STEIN, R. B. The frequency of nerve action potentials generated by applied currents. *Proc. R. Soc. Lond. B Biol. Sci.* 167: 64–86, 1967a.

STEIN, R. B. Some models of neuronal variability. *Biophys. J.* 7: 37–68, 1967b.

STERIADE, M. Synchronized activities of coupled oscillators in the cerebral cortex and thalamus at different levels of vigilance. *Cereb. Cortex* 7: 583–604, 1997.

STERIADE, M., NUÑEZ, A., AND AMZICA, F. Intracellular analysis of relations

between the slow (< 1 Hz) neocortical oscillation and other sleep rhythms of the electroencephalogram. *J. Neurosci.* 13: 3266–3283, 1993.

TANG, A. C., BARTELS, A. M., AND SEJNOWSKI, T. J. Effects of cholinergic modulation on responses of neocortical neurons to fluctuating input. *Cerebral Cortex* 7: 502–506, 1997.

THEILER, J., EUBANK, S., LONGTIN, A., GALDRIKIAN, B., AND FARMER, J. D. Testing for nonlinearity in time series: the method of surrogate data. *Physica D* 58: 77–94, 1992.

TUCKWELL, H. C. *Stochastic Processes in the Neurosciences*. Philadelphia, PA: Society for Industrial and Applied Mathematics, 1989.

VICTOR, J. D. AND PURPURA, K. P. Nature and precision of temporal coding in visual cortex: A metric-space analysis. *J. Neurophysiol.* 76: 1310–1326, 1996.

WERNER, G. AND MOUNTCASTLE, V. B. The variability of central neural activity in a sensory system, and its implications for the central reflection of sensory events. *J. Neurophysiol.* 26: 958–977, 1963.

WILBUR, J. W. AND RINZEL, J. A theoretical basis for large coefficient of variation and bimodality in neuronal interspike interval distributions. *J. Theor. Biol.* 105: 345–368, 1983.

WILSON, C. J. AND KAWAGUCHI, Y. The origins of two-state spontaneous membrane potential fluctuations of neostriatal spiny neurons. *J. Neurosci.* 16: 2397–2410, 1996.

WU, J.-Y., HOPP, H.-P., COHEN, L. B., TANG, A. C., AND FALK, C. X., Consistency in nervous systems: trial-to-trial and animal-to-animal variations in the responses to repeated applications of a sensory stimulus in *Aplysia*. *J. Neurosci.* 14: 1366–1383, 1994.